scientific reports

Check for updates

OPEN

Lysosomal Ca^{2+} release-facilitated TFEB nuclear translocation alleviates ischemic brain injury by attenuating autophagic/lysosomal dysfunction in neurons

Qian Lei[1,3], Xuemei Chen[1,3], Yajie Xiong[1], Shangdan Li[1], Jiaqian Wang[1], Hongyun He[1,2]✉ & Yihao Deng[1]✉

Neuronal death was frequently driven by autophagic/lysosomal dysfunction after ischemic stroke, whereas how to restore the impaired autophagic flux remained elusive. Autophagic/lysosomal signaling could be augmented after transcription factor EB (TFEB) nuclear translocation, which was facilitated by its dephosphorylation. A key TFEB dephosphorylase was calcineurin (CaN), whose activity was drastically regulated by cytosolic calcium ion concentration ($[Ca^{2+}]$) controlled by lysosomal Ca^{2+} channel-like protein of TRPML1. Our research shows that ML-SA1, an agonist of the TRPML1 channel, significantly enhanced the lysosomal Ca^{2+} release and the CaN expression in penumbric neurons, subsequently promoted TFEB nuclear translocation, and greatly reversed autophagy/lysosome dysfunction. Moreover, ML-SA1 treatment significantly reduced neuronal loss, infarct size, and neurological deficits. By contrast, ML-SI3, an inhibitor of TRPML1, inhibited the lysosomal Ca^{2+} release conversely, aggravated the impairment of autophagic flux and consequentially exacerbated brain stroke lesion. These studies suggest that TRPML1 elevation alleviates ischemic brain injury by restoring autophagic/lysosomal dysfunction via Lysosomal Ca^{2+} release-facilitated TFEB nuclear translocation in neurons.

Keywords Ischemic stroke, Lysosomal Ca^{2+}, Autophagic/lysosomal dysfunction, TFEB, TRPML1, Neuroprotection

Ischemic stroke is one of the major diseases that lead to deaths and disabilities in human beings[1]. There are approximately 2.7 million new stroke cases annually in China[2]. The pathogenesis of cerebral ischemia has been deeply investigated in recent decades, but valuable therapeutic clues are seldom sought[3,4]. Neuron is a type of cell with intense metabolic activity in the brain tissues and thus is highly susceptible to numerous pathological conditions, especially ischemia[5,6]. Therefore, understanding the underlying pathogenesis of ischemic neuronal injury may be an essential route to uncover novel therapies for stroke treatment.

Compelling evidence demonstrated that autophagy was extensively implicated in the pathophysiological processes of cerebral stroke[7,8]. Either excessive or insufficient autophagy was adverse to cytoprotection[9,10]. However, it was confused about what degree of autophagy benefited poststroke neuroprotection. Autophagy comprises a series of continuous processes, including autophagy initiation, formation of autophagosomes, presentation of autophagic substrates by fusion of autophagosomes with lysosomes, degradation of autophagic cargoes within autolysosomes[11,12]. A consecutive state of these processes was termed autophagic flux, as well as autophagic/lysosomal signaling pathway. On the one hand, adequate autophagy was needed to maintain homeostasis by clearance of the injured organelles, aging proteins, superfluous cytoplasmic components, etc. On the other hand, the autophagic substrates were required to be efficiently digested and degraded by autolysosomes[13]. Autophagic/lysosomal dysfunction might be created if this balance between autophagic activation and lysosomal degradation was disrupted[14,15]. Our previous study showed that neuronal autophagy was excessively activated to generate massive autophagic materials[16]. Consequently, the autophagic cargoes accumulated within neurons,

[1]School of Basic Medical Sciences, Kunming University of Science and Technology, Kunming 650500, China. [2]Anning First People's Hospital, Kunming University of Science and Technology, Kunming 650500, China. [3]These authors contributed equally: Qian Lei and Xuemei Chen. ✉email: 18487158200@163.com; deng13032871868@163.com

accompanied by lysosomal inefficiency due to digestive exhaustion. Thus, an impairment of autophagic flux was produced to exacerbate ischemic brain injury[17]. Therefore, restoring the autophagic/lysosomal dysfunction in neurons might be a protective strategy to alleviate neurological injury after ischemic stroke.

TFEB was considered a master regulator of autophagic/lysosomal signaling[18,19]. Both autophagy-related gene transcriptions and lysosome biogenesis could be concurrently promoted after TFEB nuclear translocation[20–22]. Therefore, we reasoned that the cerebral ischemia-created autophagic/lysosomal dysfunction might be restored by facilitating TFEB nuclear translocation. The subcellular localization of TFEB was determined by its phosphorylation level. The phosphorylated TFEB was retained in the cytoplasm by interaction with 14-3-3 adhesive protein[23]. After dephosphorylation, TFEB quickly entered into the nucleus to initiate the CLEAR (coordinated lysosomal expression and regulation) signaling, which consequently augmented lysosomal biosynthesis and autophagy initiation[24,25]. This suggested that attenuating TFEB phosphorylation was an effective approach to alleviate the autophagic/lysosomal dysfunction in ischemic neurons. A key TFEB dephosphorylase was calcineurin (CaN)[26,27], whose activity was positively regulated by cytosolic [Ca^{2+}]. The study indicated that Ca^{2+}-activated CaN could be directly bound to TFEB for dephosphorylation and efficiently boosted TFEB nuclear translocation[28]. Thus, controlling Ca^{2+} release from the Ca^{2+} store organelles became crucial to regulate CaN expression.

Investigation showed that lysosome was a Ca^{2+} signaling center, being an organelle with a high level of [Ca^{2+}] in cytosol[29]. Ca^{2+} ions within lysosomes were mostly supplemented by endoplasmic reticulum (ER) through its Ca^{2+} channels[30]. While lysosomal Ca^{2+} release was mainly mediated by a Ca^{2+} channel-like protein of mucolipin 1 (MCOLN1), as well as a member of the transient receptor potential channel family 1 (TRPML1)[29,31]. The study demonstrated that TRPML1-mediated Ca^{2+} release greatly evoked local calcium signaling, which effectively activated CaN for TFEB dephosphorylation[28]. To investigate the correlation between TRPML1 expression and CaN expression under ischemia conditions, a rat model of ischemic stroke was established in our preliminary experiment. We found that TRPML1 expression at the penumbra was significantly decreased, coupling with prominently suppressed CaN expression 48 h after the insult. At this time point, a serious autophagic/lysosomal dysfunction was observed. Accordingly, we hypothesized that TRPML1 was inhibited to reduce lysosomal Ca^{2+} release, leading to CaN inhibition. Subsequently, TFEB nuclear translocation was attenuated to down-regulate autophagic/lysosomal signaling[32]. This might be the pathogenesis of autophagic/lysosomal dysfunction in neurons after ischemic stroke.

Based on the regulative effect of TRPML1 on autophagic/lysosomal signaling[33–35], this study was to investigate whether the autophagic/lysosomal dysfunction in ischemic neurons could be restored by elevating TRPML1-mediated Ca^{2+} release. The rat model of MCAO and HT22 neuron ischemia model of OGD were prepared, respectively. TRPML1 channels were altered by its agonist ML-SA1 and inhibitor ML-SI3 [36,37], respectively. After that, the penumbic tissues and OGD HT22 neurons were obtained to detect CaN expression, nuclear and cytoplasmic TFEB, and the key proteins in the autophagic/lysosomal signaling pathway. By this study, the regulative machinery of TRPML1 on autophagic flux was to be revealed in ischemic neurons. Meanwhile, the neuroprotective mechanism of TRPML1 elevation in alleviating post-stroke injury was elucidated.

Results

Ischemia-blocked TRPML1 channels inhibited CaN expression in neurons

The dynamic variations between TRPML1 and calcineurin (CaN) expressions were investigated after ischemia. Western blot (Fig. 1A,D) showed that both TRPML1 (Fig. 1B) and CaN (Fig. 1C) expressions at the penumbra were prominently reduced 48 h after MCAO/reperfusion. Similarly, the significantly attenuated TRPML1 (Fig. 1E) expression was coupled with inhibited CaN (Fig. 1F) expression in HT22 neurons 1 h after OGD. Moreover, immunofluorescence (Fig. 1G) demonstrated that the cerebral ischemia-inhibited TRPML1 (Fig. 1H,I) channels and CaN (Fig. 1J,K) expression were predominantly displayed in neurons at the penumbra. Thus, the characteristic time points were identified to be 48 h after MCAO as well as 1 h after OGD, concerning the relevant changes between TRPML1 channels and CaN expression after ischemia.

Elevating TRPML1 channels greatly enhanced CaN expression in ischemic neurons

ML-SA1 and ML-SI3 are the potent membrane-permeable specific agonist and inhibitor, which serve as useful chemical tools to study the function of TRPML1[38–41]. Based on the characteristic time points after the ischemia, TRPML1 (Fig. 2A–C,E,G,H,K) channels were altered by treatment with agonist ML-SA1 and inhibitor ML-SI3, respectively. The results indicated that cytosolic [Ca^{2+}] (Fig. 2G,J) within HT22 neurons was greatly promoted to reinforce CaN (Fig. 2B,F,G,L) expression in OGD + ML-SA1 group, compared with those in OGD group. Conversely, ML-SI3-inhibited TRPML1 significantly reduced Ca^{2+} (Fig. 2G,J) release, resulting in inactivation of CaN (Fig. 2B,F,G,L). Similarly, the [Ca^{2+}] within penumbral neurons was not directly detected, but CaN (Fig. 2G,I) expression at the penumbra was greatly promoted by ML-SA1.

TRPML1 up-regulation significantly boosted TFEB nuclear translocation

The cytoplasmic and nuclear TFEB were detected to evaluate its subcellular localization 48 h after MCAO, as well as 1 h after OGD. Western blot demonstrated that TFEB (Fig. 3A–C) expression in the nucleus was increased in the MCAO + ML-SA1 group, compared with that in the MCAO group. Similarly, the nuclear TFEB (Fig. 3D–F) expression was prominently promoted by ML-SA1 but conversely reduced by ML-SI3 in OGD HT22 neurons. Meanwhile, immunofluorescence showed that ML-SA1 significantly promoted the percentage of NeuN-positive cells co-labeled with TFEB and DAPI, but barely affected the ratio of that in NeuN-negative cells (Fig. 3G,I,J). Moreover, the fluorescence intensity co-stained with TFEB and DAPI was also enhanced in the OGD + ML-SA1 group, compared with that in the OGD group (Fig. 3H,K).

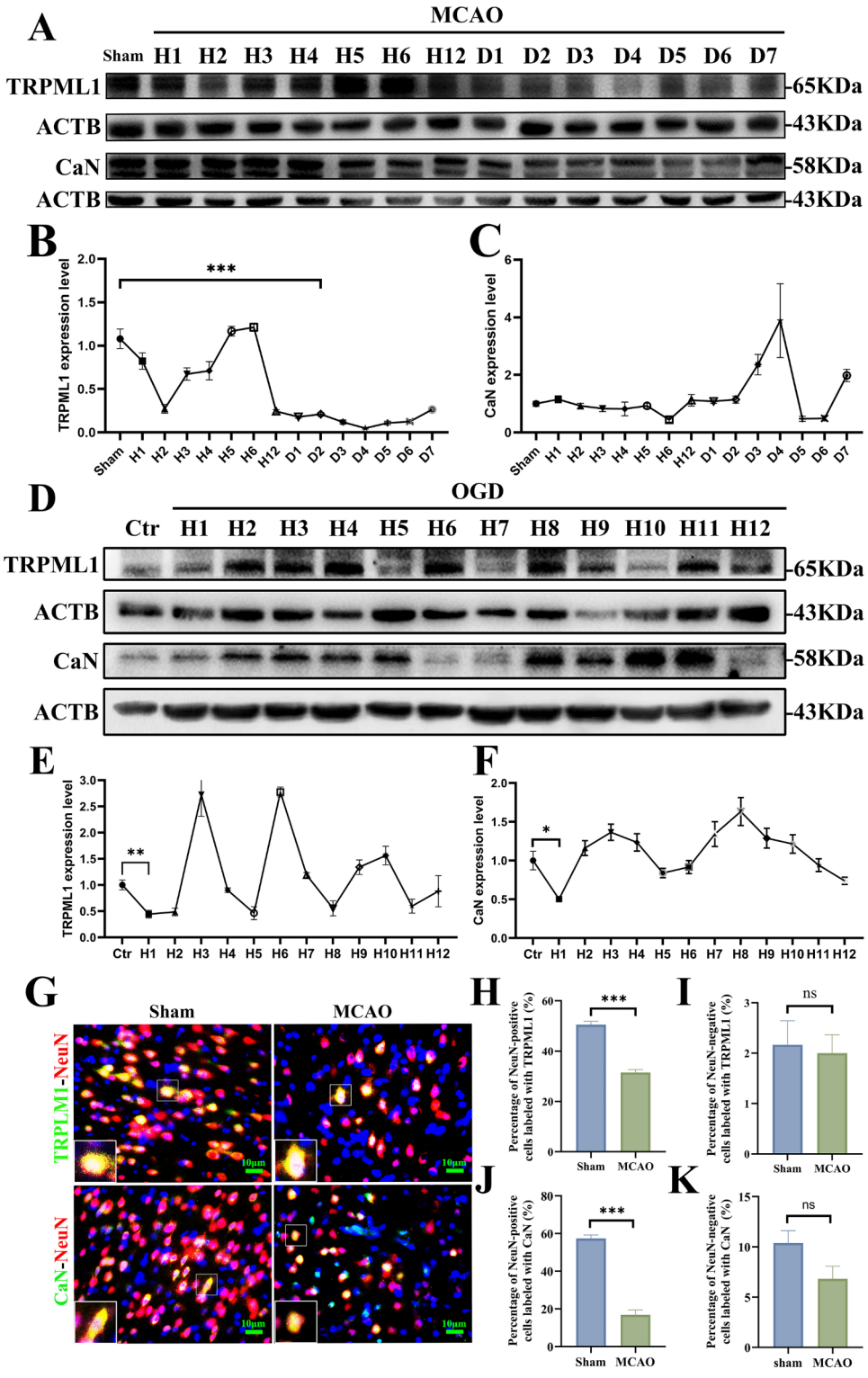

Fig. 1. The correlative changes between TRPML1 expression and CaN expression were investigated after ischemia. (**A**, **B**, **C**) Western blot demonstrated that TRPML1 channels were greatly blocked, resulting in inhibited CaN expression in penumbral tissues 48 h after MCAO, (**D**, **E**, **F**) as well as in HT22 neurons 1 h after OGD. Images were cropped, and full-length blots are presented in Supplementary Information. (**G**, **H**, **I**, **J**, **K**) Immunofluorescence showed that the down-regulated TRPML1 channels and CaN expression were mainly displayed in neurons at the penumbra. $n = 6$. $^{*}p < 0.05$, $^{**}P < 0.01$, $^{***}p < 0.001$; ns, $p > 0.05$.

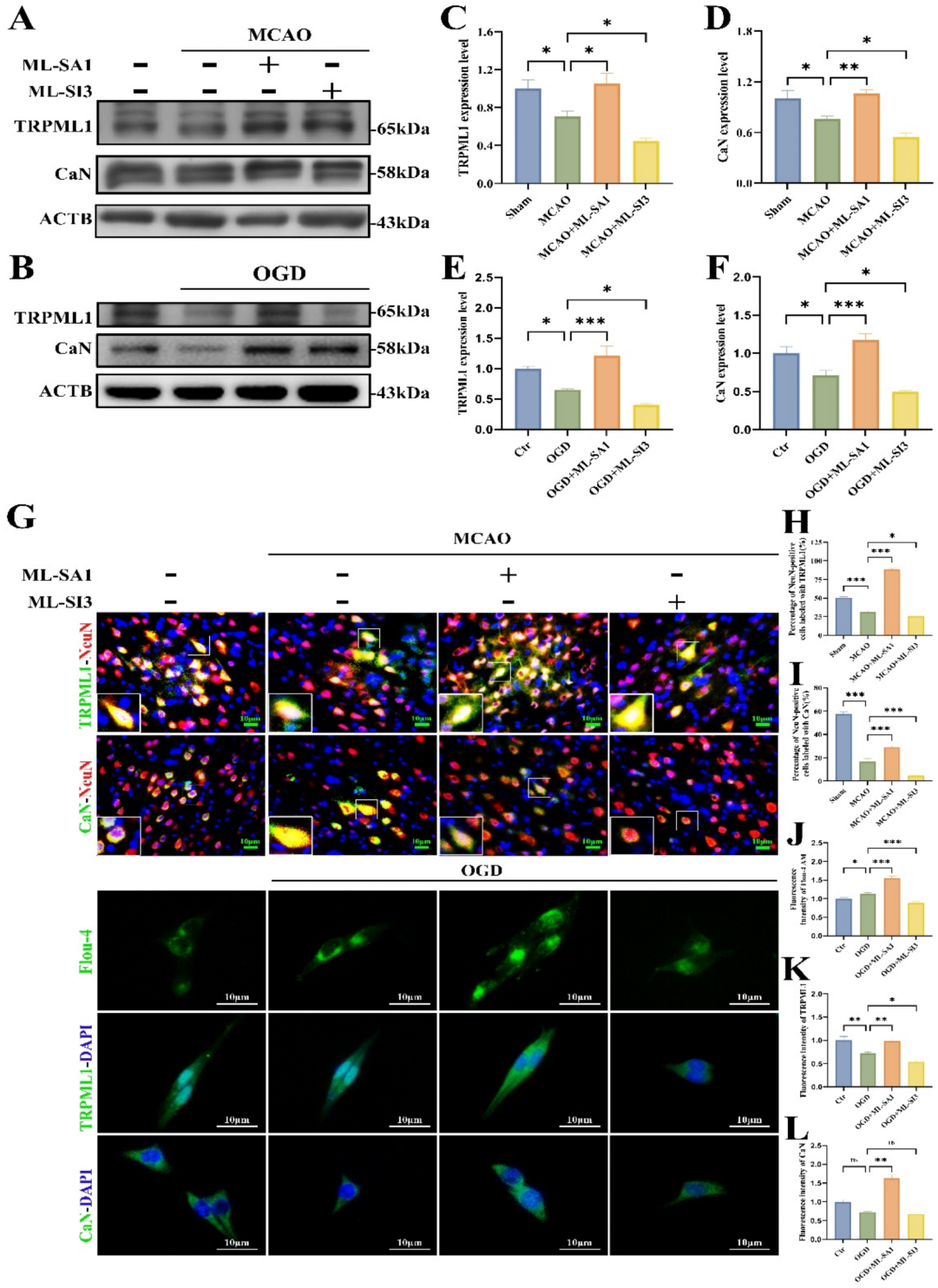

Fig. 2. Up-regulating TRPML1 drastically reinforced CaN expression by promoting cytosolic [Ca^{2+}] in ischemic neurons. (**B**, **E**, **F**, **G**, **J**, **K**, **L**) ML-SA1-augmented TRPML1 channels efficiently promoted cytosolic [Ca^{2+}], leading to enhanced CaN expression in OGD HT22 neurons. Similarly, (**A**, **C**, **D**, **G**, **H**, **I**) CaN expression in penumbral tissues could also be effectively promoted by TRPML1 agonist ML-SA1. Images were cropped, and full-length blots are presented in Supplementary Information. $n = 6$. $^{*}p < 0.05$, $^{**}p < 0.01$, $^{***}p < 0.001$; ns, $p > 0.05$.

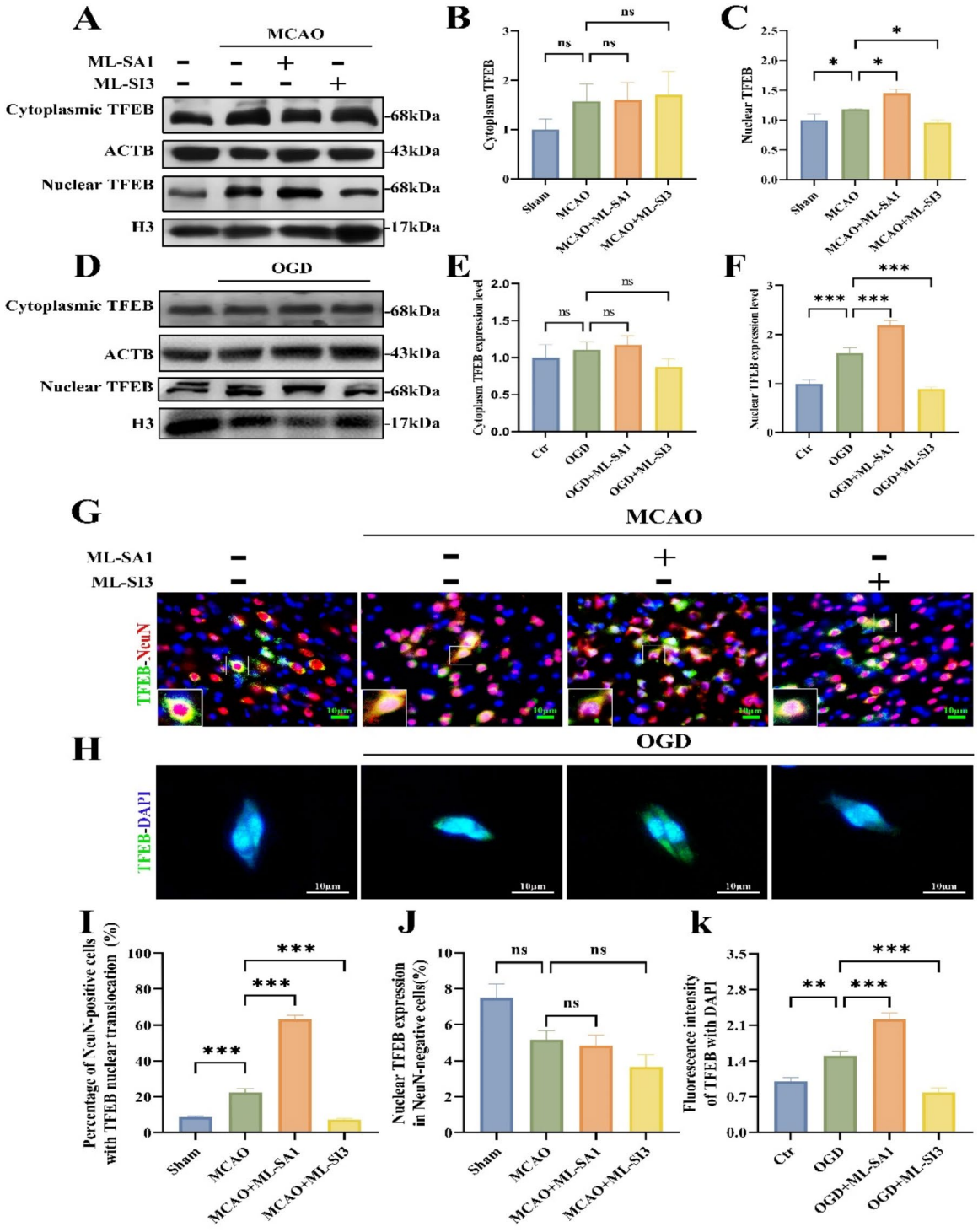

Fig. 3. TRPML1 elevation markedly facilitated TFEB nuclear translocation in ischemic neurons. (**A**, **B**, **C**, **D**, **E**, **F**) ML-SA1 treatment strongly boosted TFEB nuclear translocation in either penumbral neurons or OGD HT22 cells, as indicated by its increased expression in the nucleus. Images were cropped, and full-length blots are presented in Supplementary Information. (**G**, **I**, **J**) This was also validated by the promoted NeuN-positive cells co-labeled with TFEB and DAPI in penumbral tissues, (**H**, **K**) as well as enhanced fluorescence intensity of TFEB co-stained with DAPI in OGD HT22 neurons. $n = 6$. $^{*}p < 0.05$, $^{**}P < 0.01$, $^{***}p < 0.001$; ns, $p > 0.05$.

TRPML1 elevation effectively alleviated autophagic/lysosomal dysfunction after ischemic stroke

To investigate the effects of TRPML1 channels on autophagic flux, the key proteins in the autophagic/lysosomal signaling pathway were detected 48 h after MCAO. The results showed that the autophagic substrates of LC3-II, insoluble SQSTM1, and ubiquitinated proteins in the penumbral tissues were markedly attenuated, accompanying by promoted lysosomal CTSD in the MCAO + ML-SA1 group, compared with those in MCAO group (Fig. 4A–F). Moreover, immunofluorescence confirmed that the MCAO-induced lysosomal inefficiency was greatly resumed by the increased number of cells co-stained with SQSTM1 and CTSD. By contrast, ML-SI3-downregulated TRPML1 conversely aggravated the impairment of autophagic flux in penumbral tissues (Fig. 4G,H).

TRPML1 up-regulation dramatically resumed autophagic flux in HT22 neurons after OGD

HT22 neurons were collected to evaluate the state of autophagic flux 1 h after OGD. After treatment with TRPML1 agonist ML-SA1, the OGD-created autophagic/lysosomal dysfunction was significantly restored, as shown by reduced autophagic cargoes (Fig. 5A–F). Meanwhile, the immunofluorescence intensity labeled with SQSTM1-CTSD and LysoSensor was greatly enhanced, indicating the OGD-driven lysosomal inefficiency was greatly reversed by TRPML1 up-regulation (Fig. 5G–I). Comparatively, the autophagic/lysosomal dysfunction was conversely exacerbated in the OGD + ML-SI3 group, compared with that in the OGD group.

Facilitating TRPML1 channels prominently promoted neuron survival

Nissl staining, double immunofluorescence, and FJC staining were performed to evaluate neuron survival, respectively. The number of Nissl bodies and NeuN-positive cells at the penumbra was significantly promoted, whereas the FJC-labeled cells were conversely reduced in the MCAO + ML-SA1 group, compared with those in the MCAO group (Fig. 6A–D). Similarly, TRPML1 facilitation also conferred cytoprotection against OGD in HT22 neurons, as indicated by increased Nissl bodies and cell viability. Conversely, suppressing TRPML1 channels oppositely exacerbated neuron loss in the penumbric area, as well as in OGD HT22 neurons (Fig. 6A,E–G).

Boosting TRPML1 channels markedly mitigated the neurological deficits and infarct size after ischemic stroke

The mNSS test was performed to evaluate neurological deficits and the infarct size was measured by TTC staining 48 h after MCAO/reperfusion (Fig. 7A–C). The results showed that the neurological deficits and the infarct area were significantly attenuated by TRPML1 agonist ML-SA1 but were conversely aggravated by its inhibitor ML-SI3, suggesting augmenting TRPML1 channels benefited restoration of neurological functions after cerebral ischemia.

Discussion

The correlative changes between TRPML1 channels and CaN expression were first investigated after cerebral ischemia. The results indicated that the significantly decreased TRPML1 expression was coupled with prominently inhibited CaN expression at the penumbra 48 h after MCAO, as well as in HT22 neurons 1 h after OGD (Fig. 1A–F). At these time points, an autophagic/lysosomal dysfunction was observed, as demonstrated by the increased autophagic substrates of LC3-II, insoluble SQSTM1 and ubiquitinated proteins, coupling with lysosomal inefficiency (Figs. 4A–F and 5A–F). Thus, we assumed that the cerebral ischemia-inactivated TRPML1 led to reduced lysosomal Ca^{2+} release, which subsequently inhibited CaN expression[42]. Consequently, TFEB dephosphorylation was reduced to prevent its nuclear translocation, resulting in down-regulated autophagic/lysosomal signaling[43]. This be a pathological mechanism that drove the autophagic/lysosomal dysfunction in neurons after ischemic stroke[44]. Accordingly, we discussed whether the impaired autophagic flux could be restored by promoting TRPML1-mediated Ca^{2+} release.

After treatment with the agonist ML-SA1, TRPML1 expression was effectively promoted in both penumbric tissues and in vitro HT22 neurons (Fig. 2A–F). Immunofluorescence showed that ML-SA1-altered TRPML1 was predominantly displayed in neurons at the penumbra (Fig. 2G,H). There was a lack of methods to detect $[Ca^{2+}]$ within penumbral neurons, but enhanced CaN expression (Fig. 2G,I) was detected after treatment with ML-SA1. By contrast, the cytosolic $[Ca^{2+}]$ in OGD HT22 neurons was directly detected to promote, leading to reinforced CaN expression in the OGD + ML-SA1 group, compared with those in the OGD group. Conversely, ML-SI3-inhibited TRPML1 prominently suppressed CaN expression due to reduced cytosolic $[Ca^{2+}]$ (Fig. 2G,J–L). This indicated that TRPML1-controlled cytosolic $[Ca^{2+}]$ tightly regulated CaN expression in ischemic neurons[45]. Theoretically, ML-SA1-reinforced CaN expression could greatly boost TFEB nuclear translocation by attenuating its phosphorylation. However, there were multiple phosphorylated sites on TFEB, it was still unclear which phosphorylated sites were responsible for nuclear translocation, as well as cytosolic retention[46]. Therefore, the TFEB phosphorylation level was not assessed in our study. Instead, the cytoplasmic and nuclear expressions were respectively detected to evaluate TFEB subcellular localization[47]. Western blot demonstrated that TFEB expression in nucleus was increased in OGD + ML-SA1 group, compared with those in OGD group (Fig. 3D–F). Similarly, ML-SA1 treatment prominently promoted the percentage of NeuN-positive cells co-labeled with TFEB and DAPI in penumbral tissues (Fig. 3G,I). These data indicated ML-SA1-reinfored CaN expression greatly facilitated TFEB nuclear translocation.

To investigate the effect of ML-SA1-boosted TFEB nuclear translocation on autophagic flux, the key proteins in the autophagic/lysosomal signaling pathway were detected[48]. The results showed that both autophagic activity and lysosomal capacity were concurrently augmented in the MCAO + ML-SA1 group, compared with those in the MCAO group (Fig. 4A,B,F). Similarly, ML-SA1 also markedly enhanced the autophagic signaling in OGD

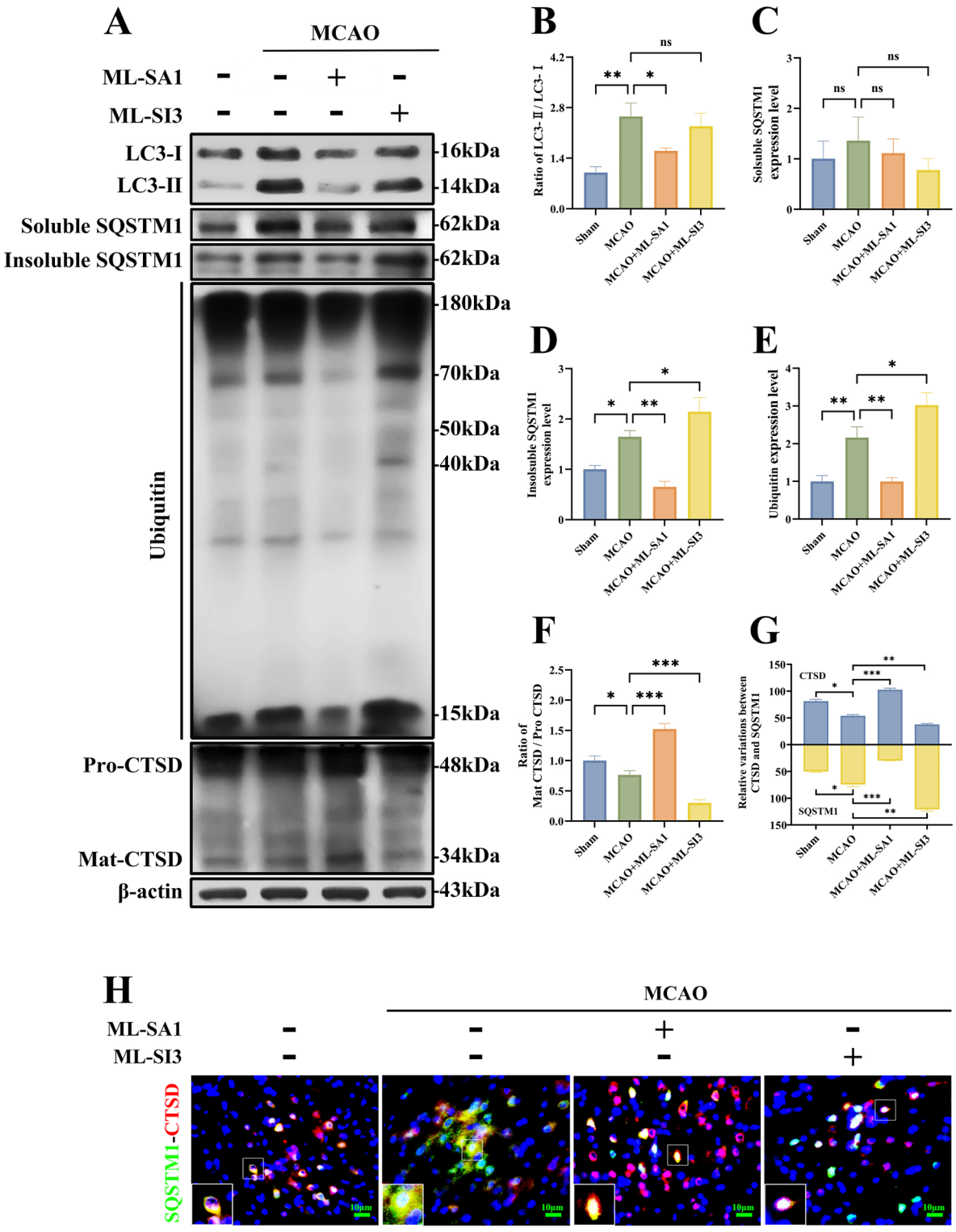

Fig. 4. Augmenting TRPML1 channels significantly alleviated the autophagic/lysosomal dysfunction at the penumbra after MCAO. (**A**, **B**, **C**, **D**, **E**, **F**) TRPML1 up-regulation greatly ameliorated the autophagic flux at the penumbra, as reflected by decreased LC3-II, insoluble SQSTM1 and ubiquitinated proteins. Images were cropped, and full-length blots are presented in Supplementary Information. (**G**, **H**) Meanwhile, the lysosomal functions were prominently enhanced, as indicated by the increased cells co-labeled with SQSTM1 and CTSD in penumbral tissues. $n = 6$. $^{*}p < 0.05$, $^{**}p < 0.01$, $^{***}p < 0.001$; ns, $p > 0.05$.

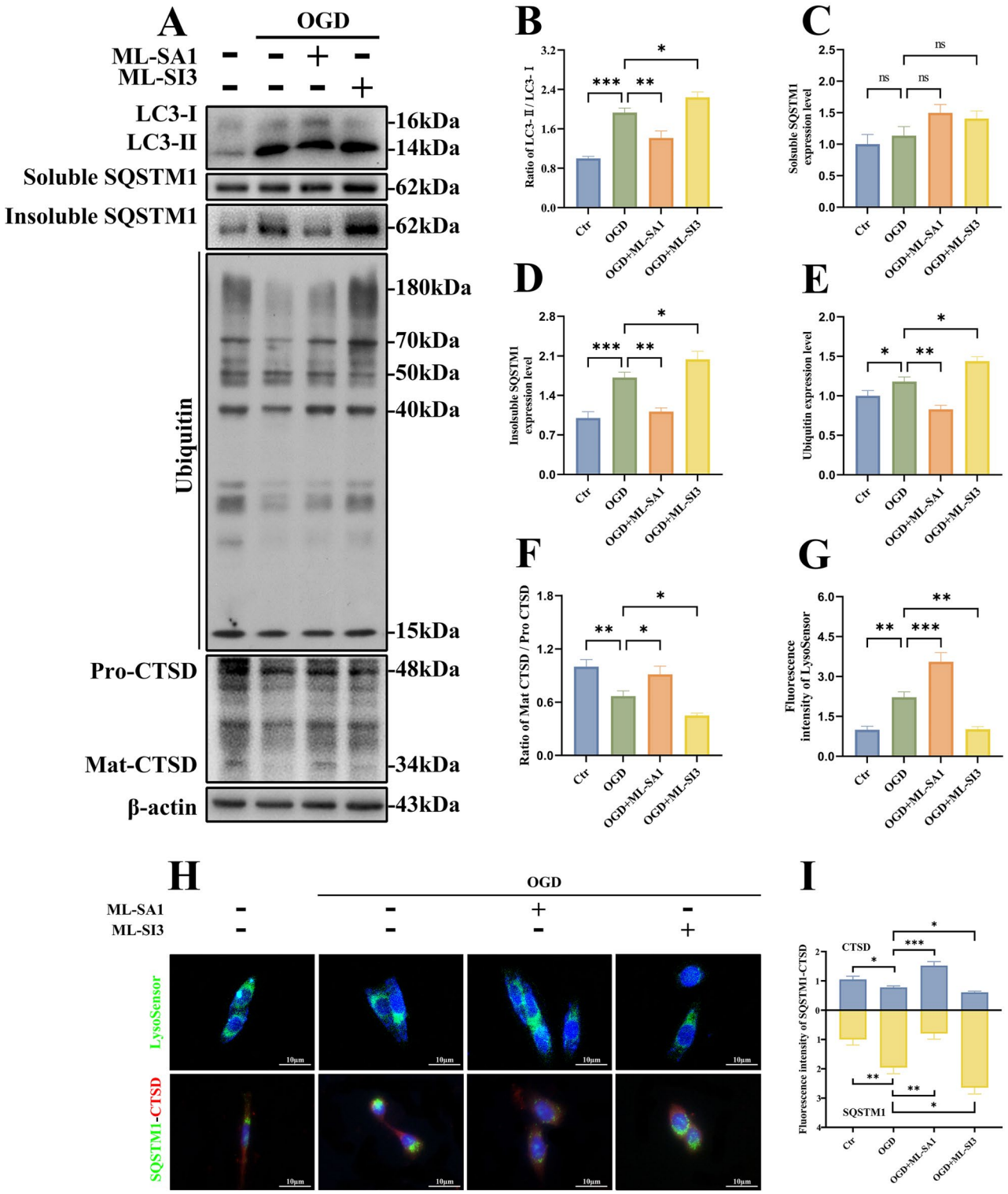

Fig. 5. Reinforcing TRPML1 channels markedly ameliorated autophagic flux in HT22 neurons after OGD. (**A**, **B**, **C**, **D**, **E**, **F**, **G**, **H**, **I**) Treatment with TRPML1 agonist ML-SA1 effectively restored the OGD-driven autophagic/lysosomal dysfunction, as shown by reduced autophagic substrates and augmented lysosomal functions. Images were cropped, and full-length blots are presented in Supplementary Information. $^{*}p < 0.05$, $^{**}p < 0.01$, $^{***}p < 0.001$; ns, $p > 0.05$.

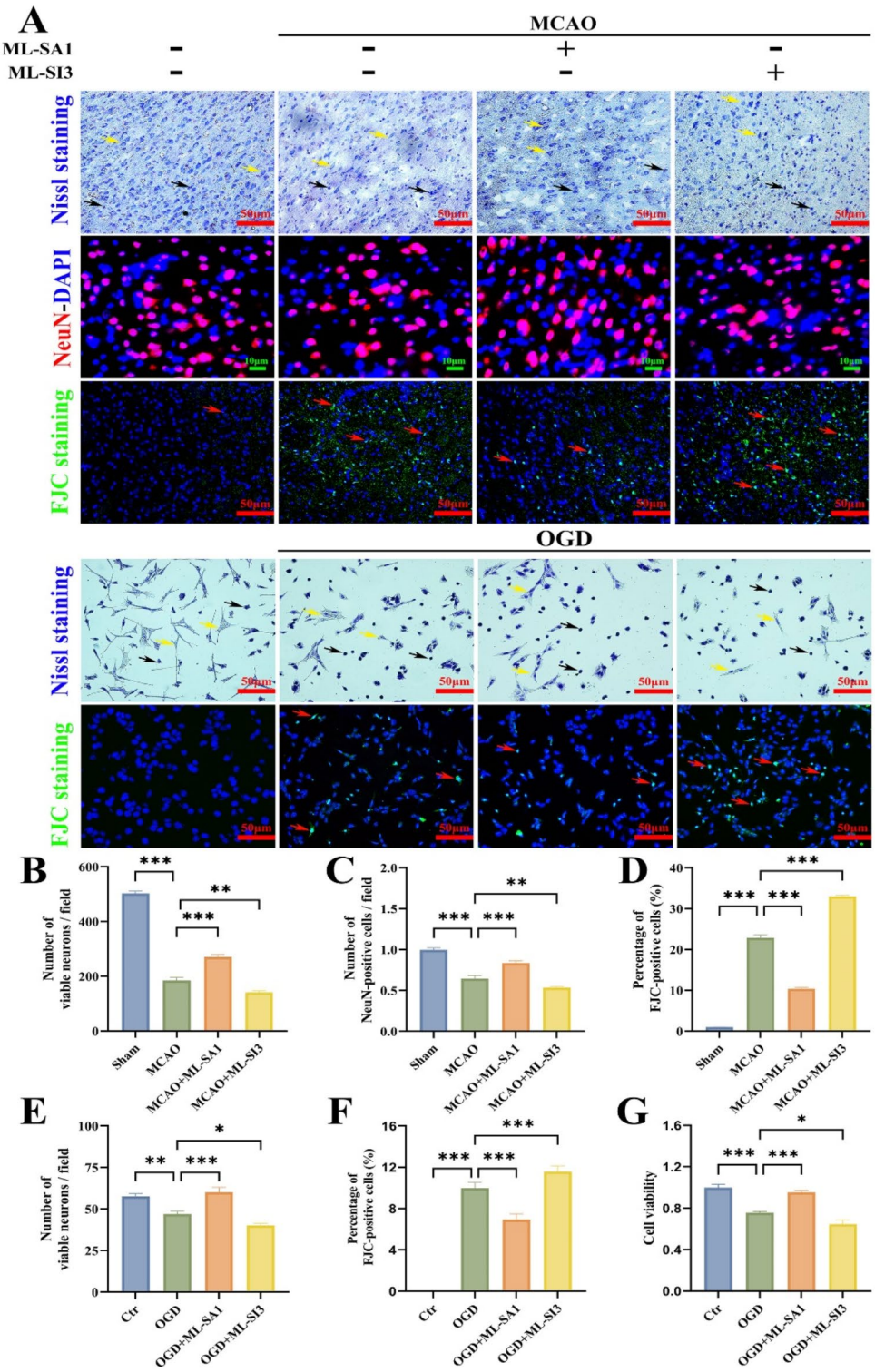

Fig. 6. Facilitating TRPML1 channels greatly promoted neuron survival after ischemia. (**A**, **B**, **C**, **D**, **E**, **F**, **G**) The number of Nissl bodies, NenN-positive cells, and viable neurons was dramatically promoted by TRPML1 agonist ML-SA1 in the penumbral area, as well as in OGD HT22 neurons. By contrast, TRPML1 inhibitor ML-SI3 conversely increased neuron death. $n = 6$. $^{*}p < 0.05$, $^{**}p < 0.01$, $^{***}p < 0.001$; ns, $p > 0.05$.

HT22 neurons, as indicated by promoted expressions of LC3-II and lysosomal CTSD (Fig. 5A,B,F). The ML-SA1-elevated autophagic activity necessarily increased the generation of autophagic substrates. However, the autophagic materials of insoluble SQSTM1 and ubiquitinated proteins were not accumulated but conversely reduced in the MCAO + ML-SA1 group, as well as in the OGD + ML-SA1 group (Figs. 4 and 5A,C–F). This

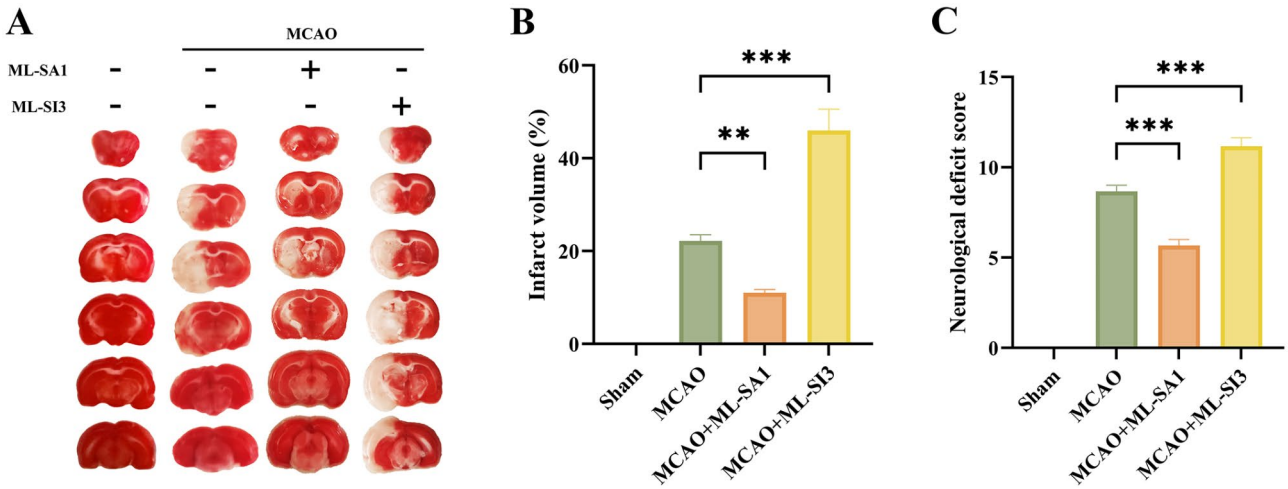

Fig. 7. TRPML1 up-regulation reduced the infarct size and the neurological deficits after ischemic stroke. (**A**, **B**) The infarct volume was measured by TTC staining. The infarct area was significantly attenuated by TRPML1 up-regulation in MCAO + ML-SA1, compared with that in the MCAO group. (**C**) The neurological deficiency was largely restored by TRPML1 up-regulation but conversely exacerbated by TRPML1 inhibitor ML-SI3. $n = 6$. $^{*}p < 0.05$, $^{**}p < 0.01$, $^{***}p < 0.001$; ns, $p > 0.05$.

implied that ML-SA1-increased autophagic cargoes could efficiently degrade lysosomes. Moreover, the ratio of cells co-labeled with SQSTM1 and CTSD was significantly promoted in the MCAO + ML-SA1 group (Fig. 4G,H), confirming lysosomal capacity was greatly augmented by ML-SA1-facilitated TFEB nuclear translocation. Collectively, these data supported that cerebral ischemia-driven autophagic/lysosomal dysfunction in neurons could be effectively restored by TFEB nuclear translocation, which was boosted by elevating TRPML1 channels.

The neurological deficits, infarct size, and neuron death were dramatically attenuated in the MCAO + ML-SA1 group, compared with those in the MCAO group (Fig. 7). This indicated that TRPML1 agonist ML-SA1 could effectively alleviate the ischemic brain injury. Moreover, this neuroprotective effect was also validated in vitro OGD HT22 neurons, as shown by improved cell viability and neuron survival in the OGD + ML-SA1 group, compared with those in the OGD group. By contrast, TRPML1 inhibitor ML-SI3 conversely aggravated the ischemic injury in both MCAO rats and OGD HT22 neurons. ML-SA1 could significantly enhance TRPML1-mediated lysosomal Ca^{2+} release, thereby promoting autophagy, alleviating neuron injury and neurological dysfunction that occur after ischemic stroke[49]. The main findings of this study are that the elevation of TRPML1 by ML-SA1 to ameliorate neuronal damage after ischemic stroke is achieved through promoting TFEB nuclear translocation (Fig. 8).

Taken together, our study demonstrates that TRPML1 elevation alleviated post-stroke injury by restoring autophagic/lysosomal dysfunction via the facilitation of TFEB nuclear translocation in neurons. Therefore, regulating the elevation of the lysosomal Ca^{2+} by TRPML1 to promote TFEB nuclear translocation offers a potential approach for the treatment of ischemic stroke.

Materials and methods

Ethics statement

In this study, all authors complied with the ARRIVE guidelines. All animal experiments were approved by the Animal Experimentation Committee of Kunming University of Science and Technology (approval number: 5301002013655) and all experiments methods were performed guidelines and regulations.

Experimental animals

Adult pathogen-free male Sprague Dawley rats (8–10 weeks old) were purchased from Hunan Slack Laboratory Animal Company (license number: SCXK2016-0002, Changsha, China). Under standard feeding conditions, 4–5 rats were housed in each cage with free access to food and water, under a 12 h light / 12 h dark cycle at 22 ± 1 °C. A total of 84 rats were recruited in this study and 12 rats died during and after MCAO surgery (the mortality was approximately 14.29%), the rest 72 rats were randomly divided into 4 groups: Sham group, MCAO group, MCAO + ML-SA1 (a TRPML1 agonist) group and MCAO + ML-SI3 (a TRPML1 inhibitor) group. Forty-eight hours after reperfusion, the rats were euthanized by cervical dislocation under 3% isoflurane anesthesia, then the brains were collected immediately.

Rat model of ischemic stroke was prepared by middle cerebral artery occlusion (MCAO)

The MCAO surgery was established according to our previous study[50]. Briefly, rats were anesthetized by administering an intraperitoneal injection with 2% sodium pentobarbital (50 mg/kg, Sigma-Aldrich, St.Louis, MO, USA). The left internal carotid artery (ICA), external carotid artery (ECA), and common carotid artery (CCA) were isolated, respectively. Thereafter, a nylon monofilament (Cinontech, Beijing, China) coated with a

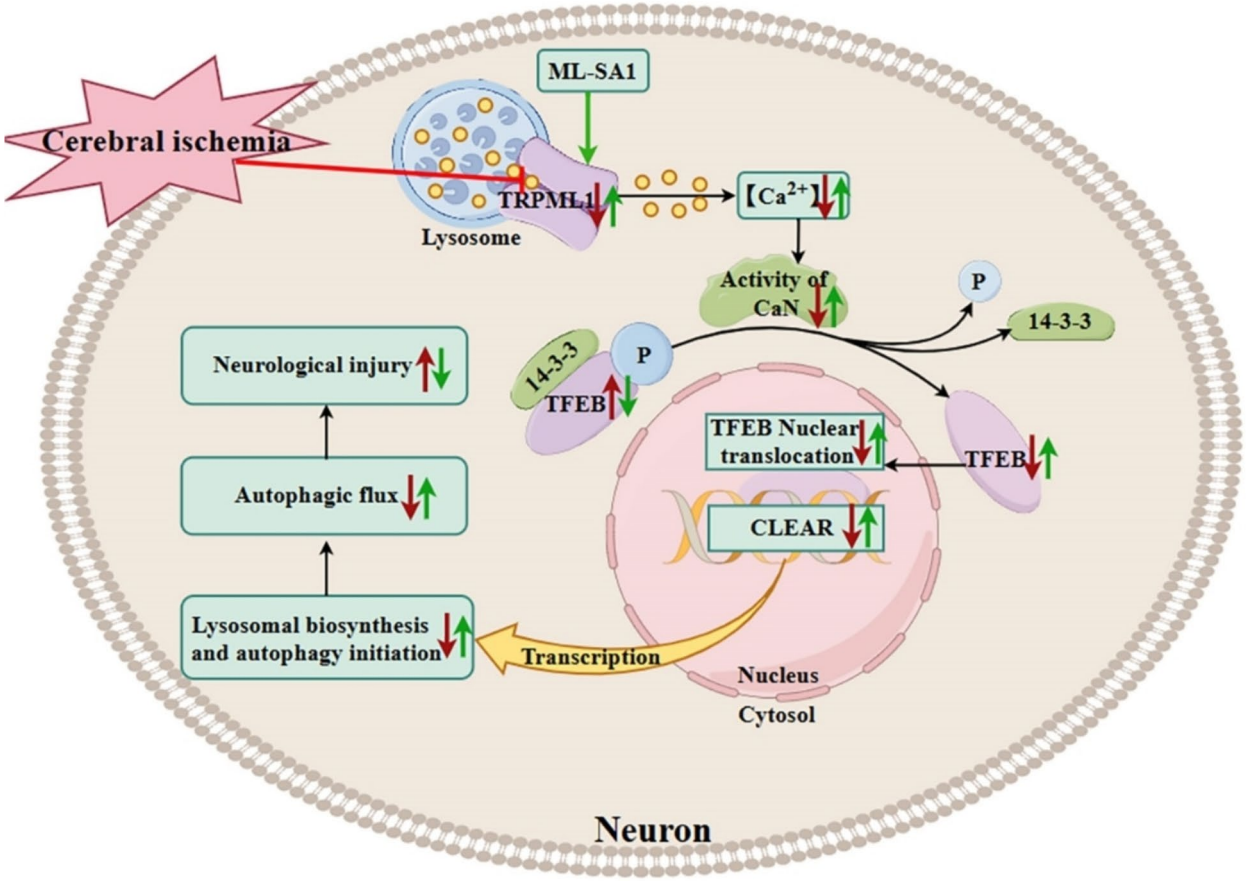

Fig. 8. Mechanism diagram of elevating TRPML1 channels ameliorates autophagic flux to alleviate ischemic neuronal injury.

round tip of silicone gel (with an approximately 0.36 mm diameter) was inserted into the CCA through a small incision on the ECA. The nylon monofilament was then introduced back into ICA and further advanced about 2 cm to reach the middle cerebral artery for occlusion (MCAO). After 90 min of MCAO, the monofilament was gently withdrawn for reperfusion. The rats in the sham group underwent the same operation except for insertion with nylon monofilament.

Intracerebroventricular administration for alteration of TRPML1 channels

The method for intracerebroventricular injection was manipulated according to our previous study[17]. Briefly, the rats were fixed on a stereotaxic apparatus (RWD Life Science Co., Ltd. Shenzhen, China) after anesthesia with 2% sodium pentobarbital. The skin and fascia of the cranial vault were excised to expose bregma, and the injection point was coordinated at 0.8 mm posterior to the bregma and 1.2 mm from the midline, a 12 mm-long cannula with a diameter of 0.6 mm was vertically inserted 3.5 ~ 3.8 mm into the left lateral ventricle and a solid pin with 0.15 mm of diameter was inserted to seal the cannula. The agents were administrated to alter TRPML1-mediated lysosomal Ca^{2+} release by intracerebroventricular injection. Both TRPML1 agonist ML-SA1 (0.144 mg/Kg, Selleck, Shanghai, China) and TRPML1 inhibitor ML-SI3 (26 μg/μL, Selleck, Shanghai, China) were treated once daily for 3 days before MCAO surgery[49], and were administrated once again after onset of reperfusion following MCAO.

The neuronal ischemia model was prepared by oxygen-glucose deprivation (OGD) in HT22 cells

Mouse hippocampal neuronal cell line (HT22) were purchased from Wuhan Purcell Life Sciences (Wuhan, China) and cultured in RPMI-1640 medium (Biosharp, Chengdu, China) containing 10% fetal bovine serum (Biological Industries, CT, USA) and 1% penicillin/streptomycin at 37 °C, with conditions of 5% CO_2[51]. To establish the oxygen-glucose deprivation (OGD) model, HT22 neurons were removed into an incubator with 5% CO_2 and 95% N_2 (oxygen deprivation) and cultured with a medium deleting glucose and serum (glucose deprivation). After 60 min of OGD, the culture medium was replaced by a complete RPMI-1640 containing 10% fetal bovine serum. Meanwhile, cells were cultured under conditions of 37 °C and 5% CO_2 (reoxygenation). Thus, the neuronal ischemia model of OGD/reperfusion was established. HT22 cells in the control group were treated identically except for OGD. Cells were randomly divided into 4 groups: Ctr group, OGD group, OGD +

ML-SA1 (20 μM[52], Selleck, Shanghai, China) group, and OGD + ML-SI3 (10 μM[53], Selleck, Shanghai, China) group.

Western blot was performed to investigate the effects of TRPML1 channels on autophagic flux in ischemic neurons

The penumbric tissues and HT22 cells were collected 48 h after MCAO, as well as 1 h after OGD. The proteins were extracted by a Nuclei and Cytoplasmic Protein Extraction Kit (Beyotime, Shanghai, China) and were measured for protein concentrations with a BCA Protein Concentration Assay Kit (Beyotime, Shanghai, China). The proteins with different molecular weights were separated by sodium dodecyl sulfate-polyacrylamide gel electrophoresis (SDS-PAGE) and transferred onto polyvinylidene fluoride (PVDF, Millipore, Billerica, MA, USA) membranes. After blocking with 10% nonfat milk, the primary antibodies were incubated overnight at 4 °C, including rabbit antibodies against rat TRPML1 (1:1000, Alomone Labs, ACC-081, Jerusalem, Israel), CaN (1:1000, Thermo Fisher Scientific, PA5-29255, MA, USA), TFEB (1:1000, Thermo Fisher Scientific, PA5-96632, MA, USA), Beclin1 (1:20000, Thermo Fisher Scientific, RA5-95065, MA, USA), LC3 (1:5000, Sigma-Aldrich, L7543, St. Louis, MO, USA), SQSTM1/P62 (1:10000, Abcam, AB109012, Cambs, UK), ubiquitin (1:1000, Proteintech, 10201-2-AP, Wuhan, China), lysosome-associated membrane protein 2 (LAMP2, 1:2000, Sigma-Aldrich, L0668, St. Louis, MO, USA), β-actin (1:10000, ABclonal, AC026, Wuhan, China) and Histone H3 (1:1000, Affinity Biosciences, AF0863, California, USA), and mouse primary antibody against rat cathepsin D (CTSD, 1:1000, Abcam, AB302649, Cambs, UK). After washing, the PVDF membranes were labeled with corresponding secondary antibodies for 1 h. After washing, the immune reactions were visualized by electrochemiluminescence (ECL). Experimental results obtained using ImageJ analysis. The results were expressed as the fluorescence signal intensity normalized to β-actin or H3.

Immunofluorescence was performed to reveal the efficacy of TRPML1 channels on TFEB-regulated autophagic/lysosomal signaling

Rats were anesthetized with 2% pentobarbital sodium, and then sequentially perfused with saline and 4% paraformaldehyde (Invitrogen, Carlsbad, CA, USA) via heart 48 h after MCAO. The whole brains were quickly removed and fixed in 4% paraformaldehyde for 24 h and then immersed in 30% sucrose until they sank to the bottom. Brains were sliced into 20 μm-thickness sections with a freezing microtome (SLEE, Mainz, Germany). After 1 h following OGD/reoxygenation, cells were fixed with 4% paraformaldehyde for 10 min. Thereafter, brain tissues and HT22 cells were permeabilized with 0.2% Triton X-100 (Solarbio, Beijing, China) for 10 min and blocked with 10% goat serum (Beyotime Biotechnology, Shanghai, China) for 1 h. The primary antibodies were incubated overnight at 4 °C, including NeuN (1:400, Abcam, AB177487, Cambs, UK), TRPML1 (1:200, Alomone Labs, ACC-081, Jerusalem, Israel), CaN (1:500, Thermo Fisher Scientific, PA5-29255, MA, USA), TFEB (1:400, Thermo Fisher Scientific, PA5-96632, MA, USA), LC3 (1:400, Sigma-Aldrich, L7543, St. Louis, MO, USA), SQSTM1/P62 (1:400, Abcam, AB109012, Cambs, UK), mouse primary antibodies against rat cathepsin D (CTSD, 1:400, Abcam, AB302649, Cambs, UK). After washing, the Alexa Fluor-coupled secondary antibodies (1:800, Jackson ImmunoResearch Laboratories, 111-585-045 and 111-545-045, INC. PA, USA) were labeled for 2 h in the dark and then counterstained with DPAI (1:1000; Cell Signaling Technology, 4083, Danvers, MA, USA). Finally, the reactions were observed and photographed with a fluorescence microscope (Nikon Instruments Co., Ltd., Tokyo, Japan). The results were represented as percentages of positive cells in each penumbric field for brain tissues, and fluorescence intensity for HT22 neurons under high magnification (×400).

TTC staining was performed to assess infarct volume

The whole rat brains were quickly removed 48 h after MCAO/reperfusion and frozen at -20 °C for 15 min. After that, the brains were coronally sliced into 2 mm-thickness sections. The brain sections were immediately stained with 2% of 2,3,5-triphenyl tetrazolium chloride (TTC, Solarbio, Beijing, China) solution for 30 min at 37 °C. Images were taken with a digital camera after the staining and the infarct volumes were calculated with image J. The infarct volume was expressed as $A= (A^{0}- (A^{00}-A^{'}))/A^{0}*100\%$[54]. A: infarct volume, A^{0}: contralateral hemisphere volume, A^{00}: ipsilateral hemisphere volume, $A^{'}$: measured infarct volume.

Evaluation of neurological deficits

The neurological deficits were evaluated by the modified Neurological Severity Score (mNSS) test 48 h after MCAO/reperfusion. The mNSS test comprised 4 contents[55]: reflex evaluation, motor function, balance ability, and sensory function. A possible highest score was 18, indicating the most serious neurological deficiency. The score of 0 showed no neurological deficit.

CCK-8 kit was used to detect the cell viability of OGD HT22 neurons

The cell viability was measured by a CCK-8 kit (Beyotime Biotechnology, Shanghai, China) 1 h after OGD, according to the instructions provided by the manufacturer. The cell survival rate was assessed by cell survival rate (%) = [(As-Ab)/(Ac-Ab)]×100%. As: TRPML1 intervention group, Ac: OGD group, Ab: Ctr group.

Nissl staining was utilized to evaluate neuronal survival

Brain tissues and HT22 cells were washed with PBS and then stained with a Nissl staining solution (Beyotime, Shanghai, China) for 5 min at 37 °C. After washing with distilled water, they were dehydrated with gradiently increased concentrations of ethanol. Staining was observed with a stereomicroscope (Nikon Instruments Co., Ltd., Tokyo, Japan) and photographed. The results were expressed as the number of Nissl bodies in each field under high magnification (×200).

Fluoro-Jade C (FJC) staining was performed to evaluate neuron death

Neuronal death was assessed by Fluoro-Jade C (FJC, Thermo Fisher Scientific, MA, USA) staining 48 h after MCAO and 1 h after OGD. After fixation with 4% paraformaldehyde, brain tissues, and HT22 cells were treated with solution A (sodium hydroxide) for 5 min, followed by incubation with 70% ethanol for 2 min and washing with distilled water for 2 min. Thereafter, they were incubated with working solution B (potassium permanganate) for 10 min. After washing with distilled water, they were stained with working solution C (FJC) for 10 min. After washing, they were permeabilized with xylene and photographed with a fluorescence microscope (Nikon Instruments Co., Ltd., Tokyo, Japan). The results were represented as the number of FJC-stained cells in each randomly selected non-overlapping area under high magnification (×200).

LysoSensor was used to evaluate the number of lysosomes and lysosomal capacity

LysoSensor (Yeasen, Shanghai, China) was diluted in PBS. After pre-warming at 37 °C, it was added into a culture medium with final concentrations of 2 μM. After incubation for 1 h at 37 °C in the dark, HT22 neurons were washed twice with PBS and fixed with 4% paraformaldehyde for 10 min and finally counterstained with DAPI. The staining was photographed with a fluorescence microscope (Nikon Instruments Co., Ltd., Tokyo, Japan). The results were expressed as fluorescence intensity.

Fluo-4 AM imaging for detection of cytoplasmic [Ca^{2+}]

The Fluo-4 AM (Beyotime, Shanghai, China) was used to evaluate cytoplasmic [Ca^{2+}] 1 h after OGD. Fluo-4 AM was first diluted into PBS for a working solution. The cultured HT22 neurons were incubated with 4 μM Fluo-4 AM working solution for 1 h in the dark at 37 °C. Then, the cells were washed three times with PBS. Finally, the staining was observed and photographed with a stereomicroscope (Nikon Instruments Co., Ltd., Tokyo, Japan). The results were represented as fluorescence intensity.

Statistical analysis

All data in this study were analyzed by GraphPad Prism 9 software and expressed as mean ± standard error (SEM). Western blot bands were analyzed with Image J, and data among groups were analyzed by paired t-test and Wilcoxon rank sum test. Values of $P < 0.05$ were considered statistically different.

Data availability

The data in this study are available from the corresponding author upon reasonable request.

Received: 27 May 2024; Accepted: 8 October 2024
Published online: 22 October 2024

References

1. Campbell, B. C. V., Khatri, P. *Lancet (London England)* **396**, 129–142. https://doi.org/10.1016/s0140-6736(20)31179-x (2020).
2. Ma, Q. et al. Temporal trend and attributable risk factors of stroke burden in China, 1990–2019: an analysis for the global burden of Disease Study 2019. *Lancet Public. Health* **6**, e897–e906. https://doi.org/10.1016/s2468-2667(21)00228-0 (2021).
3. Qin, C. et al. Signaling pathways involved in ischemic stroke: Molecular mechanisms and therapeutic interventions. *Signal. Transduct. Target. Therapy* **7**https://doi.org/10.1038/s41392-022-01064-1 (2022).
4. Jurcau, A. & Simion, A. Neuroinflammation in cerebral ischemia and Ischemia/Reperfusion injuries: From pathophysiology to therapeutic strategies. *Int. J. Mol. Sci.* **23** https://doi.org/10.3390/ijms23010014 (2021).
5. Shichita, T., Ooboshi, H. & Yoshimura, A. Neuroimmune mechanisms and therapies mediating post-ischaemic brain injury and repair. *Nat. Rev. Neurosci.* **24**, 299–312. https://doi.org/10.1038/s41583-023-00690-0 (2023).
6. Zhao, Y., Zhang, X., Chen, X. & Wei, Y. Neuronal injuries in cerebral infarction and ischemic stroke: from mechanisms to treatment (review). *Int. J. Mol. Med.* **49** https://doi.org/10.3892/ijmm.2021.5070 (2022).
7. Xiaoqing, S., Yinghua, C. & Xingxing, Y. The autophagy in ischemic stroke: A regulatory role of non-coding-RNAs. *Cell. Signal.* **104**, 110586. https://doi.org/10.1016/j.cellsig.2022.110586 (2023).
8. Li, J. et al. Targeting neuronal mitophagy in ischemic stroke: An update. *Burns Trauma.* **11**, tkad018. https://doi.org/10.1093/burnst/tkad018 (2023).
9. Liu, J. et al. TMEM164 is a new determinant of autophagy-dependent ferroptosis. *Autophagy* **19**, 945–956. https://doi.org/10.1080/15548627.2022.2111635 (2023).
10. Liu, S. et al. Regulator of cell death. *Cell Death Dis.* **14** https://doi.org/10.1038/s41419-023-06154-8 (2023).
11. Shu, F. et al. Epigenetic and post-translational modifications in autophagy: Biological functions and therapeutic targets. *Signal. Transduct. Target. Therapy* **8** https://doi.org/10.1038/s41392-022-01300-8 (2023).
12. Vargas, J. N. S., Hamasaki, M., Kawabata, T., Youle, R. J. & Yoshimori, T. The mechanisms and roles of selective autophagy in mammals. *Nat. Rev. Mol. Cell Biol.* **24**, 167–185. https://doi.org/10.1038/s41580-022-00542-2 (2023).
13. Ajoolabady, A. et al. Targeting autophagy in ischemic stroke: from molecular mechanisms to clinical therapeutics. *Pharmacol. Ther.* **225**, 107848. https://doi.org/10.1016/j.pharmthera.2021.107848 (2021).
14. Shi, Q., Cheng, Q. & Chen, C. The role of Autophagy in the pathogenesis of ischemic stroke. *Curr. Neuropharmacol.* **19**, 629–640. https://doi.org/10.2174/1570159x18666200729101913 (2021).
15. Ballabio, A. & Bonifacino, J. S. Lysosomes as dynamic regulators of cell and organismal homeostasis. *Nat. Rev. Mol. Cell Biol.* **21**, 101–118. https://doi.org/10.1038/s41580-019-0185-4 (2020).
16. Lingling, D., Miaomiao, Q., Yili, L., Hongyun, H. & Yihao, D. Attenuation of histone H4 lysine 16 acetylation (H4K16ac) elicits a neuroprotection against ischemic stroke by alleviating the autophagic/lysosomal dysfunction in neurons at the penumbra. *Brain Res. Bull.* **184**, 24–33. https://doi.org/10.1016/j.brainresbull.2022.03.013 (2022).
17. Zhang, Y. et al. GSK-3β inhibition elicits a neuroprotection by restoring lysosomal dysfunction in neurons via facilitation of TFEB nuclear translocation after ischemic stroke. *Brain Res.* **1778**, 147768. https://doi.org/10.1016/j.brainres.2021.147768 (2022).
18. Carling, P. J. et al. Multiparameter phenotypic screening for endogenous TFEB and TFE3 translocation identifies novel chemical series modulating lysosome function. *Autophagy* **19**, 692–705. https://doi.org/10.1080/15548627.2022.2095834 (2023).
19. Liu, Y. L. et al. Berberine alleviates ischemic brain injury by enhancing autophagic flux via facilitation of TFEB nuclear translocation. *Am. J. Chin. Med.* **52**, 231–252. https://doi.org/10.1142/s0192415x24500101 (2024).

20. Zhao, X. et al. Quercetin alleviates ethanol-induced hepatic steatosis in L02 cells by activating TFEB translocation to compensate for inadequate autophagy. *Phytother. Res.* **37**, 62–76. https://doi.org/10.1002/ptr.7593 (2023).
21. Tan, A., Prasad, R., Lee, C. & Jho, E. H. Past, present, and future perspectives of transcription factor EB (TFEB): Mechanisms of regulation and association with disease. *Cell Death Differ.* **29**, 1433–1449. https://doi.org/10.1038/s41418-022-01028-6 (2022).
22. Dang, T. T. & Back, S. H. Translation inhibitors activate autophagy master regulators TFEB and TFE3. *Int. J. Mol. Sci.* **22** https://doi.org/10.3390/ijms222112083 (2021).
23. Xu, Y. et al. YWHA/14-3-3 proteins recognize phosphorylated TFEB by a noncanonical mode for controlling TFEB cytoplasmic localization. *Autophagy* **15**, 1017–1030. https://doi.org/10.1080/15548627.2019.1569928 (2019).
24. Settembre, C. et al. TFEB links autophagy to lysosomal biogenesis. *Sci. (New York N Y)* **332**, 1429–1433. https://doi.org/10.1126/science.1204592 (2011).
25. Franco-Juárez, B. et al. TFEB; beyond its role as an autophagy and lysosomes regulator. *Cells* **11** https://doi.org/10.3390/cells11193153 (2022).
26. Tong, Y. & Song, F. Intracellular calcium signaling regulates autophagy via calcineurin-mediated TFEB dephosphorylation. *Autophagy* **11**, 1192–1195. https://doi.org/10.1080/15548627.2015.1054594 (2015).
27. Fu, X. et al. Pseudoginsenoside F11 ameliorates the dysfunction of the autophagy-lysosomal pathway by activating calcineurin-mediated TFEB nuclear translocation in neuron during permanent cerebral ischemia. *Exp. Neurol.* **338**, 113598. https://doi.org/10.1016/j.expneurol.2021.113598 (2021).
28. Medina, D. L. et al. Lysosomal calcium signalling regulates autophagy through calcineurin and TFEB. *Nat. Cell Biol.* **17**, 288–299. https://doi.org/10.1038/ncb3114 (2015).
29. Riederer, E., Cang, C. & Ren, D. Lysosomal Ion channels: What are they good for and are they druggable targets? *Annu. Rev. Pharmacol. Toxicol.* **63**, 19–41. https://doi.org/10.1146/annurev-pharmtox-051921-013755 (2023).
30. Oh, S. J., Park, K., Sonn, S. K., Oh, G. T. & Lee, M. S. Pancreatic β-cell mitophagy as an adaptive response to metabolic stress and the underlying mechanism that involves lysosomal Ca(2+) release. *Exp. Mol. Med.* **55**, 1922–1932. https://doi.org/10.1038/s12276-023-01055-4 (2023).
31. Sun, J. et al. LAMTOR1 inhibition of TRPML1-dependent lysosomal calcium release regulates dendritic lysosome trafficking and hippocampal neuronal function. *EMBO J.* **41**, e108119. https://doi.org/10.15252/embj.2021108119 (2022).
32. Shao, J., Lang, Y., Ding, M., Yin, X. & Cui, L. Transcription factor EB: A promising therapeutic target for ischemic stroke. *Curr. Neuropharmacol.* **22**, 170–190. https://doi.org/10.2174/1570159x21666230724095558 (2024).
33. Abuammar, H. et al. Ion channels and pumps in autophagy: A reciprocal relationship. *Cells* **10** https://doi.org/10.3390/cells10123537 (2021).
34. Qi, J. et al. MCOLN1/TRPML1 in the lysosome: A promising target for autophagy modulation in diverse diseases. *Autophagy* 1–11. https://doi.org/10.1080/15548627.2024.2333715 (2024).
35. Wu, L. K. et al. Artemisia leaf extract protects against neuron toxicity by TRPML1 activation and promoting autophagy/mitophagy clearance in both in vitro and in vivo models of MPP+/MPTP-induced Parkinson's disease. *Phytomed. Int. J. Phytotherapy Phytopharmacol.* **104**, 154250. https://doi.org/10.1016/j.phymed.2022.154250 (2022).
36. Zhang, M. et al. TRP (transient receptor potential) ion channel family: Structures, biological functions and therapeutic interventions for diseases. *Signal. Transduct. Target. Therapy* **8** https://doi.org/10.1038/s41392-023-01464-x (2023).
37. Somogyi, A. et al. The synthetic TRPML1 agonist ML-SA1 rescues Alzheimer-related alterations of the endosomal-autophagic-lysosomal system. *J. Cell Sci.* **136** https://doi.org/10.1242/jcs.259875 (2023).
38. Shen, D. et al. Lipid storage disorders block lysosomal trafficking by inhibiting a TRP channel and lysosomal calcium release. *Nat. Commun.* **3**, 731. https://doi.org/10.1038/ncomms1735 (2012).
39. Schmiege, P., Fine, M. & Li, X. Atomic insights into ML-SI3 mediated human TRPML1 inhibition. *Structure (London, England)* **29**, 1295–1302. https://doi.org/10.1016/j.str.2021.06.003 (2021).
40. Zhong, D. et al. Induction of lysosomal exocytosis and biogenesis via TRPML1 activation for the treatment of uranium-induced nephrotoxicity. *Nat. Commun.* **14**, 3997. https://doi.org/10.1038/s41467-023-39716-7 (2023).
41. Leser, C. et al. Chemical and pharmacological characterization of the TRPML calcium channel blockers ML-SI1 and ML-SI3. *Eur. J. Med. Chem.* **210**, 112966. https://doi.org/10.1016/j.ejmech.2020.112966 (2021).
42. Kim, H. K. et al. TMBIM6 (transmembrane BAX inhibitor motif containing 6) enhances autophagy through regulation of lysosomal calcium. *Autophagy***17**, 761–778. https://doi.org/10.1080/15548627.2020.1732161 (2021).
43. Puertollano, R., Ferguson, S. M., Brugarolas, J. & Ballabio, A. The complex relationship between TFEB transcription factor phosphorylation and subcellular localization. *EMBO J.* **37** https://doi.org/10.15252/embj.201798804 (2018).
44. Liu, Y. et al. Neuronal-targeted TFEB rescues dysfunction of the autophagy-lysosomal pathway and alleviates ischemic injury in permanent cerebral ischemia. *Autophagy* **15**, 493–509. https://doi.org/10.1080/15548627.2018.1531196 (2019).
45. Kim, M. H. et al. Peroxiredoxin 5 inhibits glutamate-Induced neuronal cell death through the regulation of calcineurin-dependent mitochondrial dynamics in HT22 cells. *Mol. Cell. Biol.* **39** https://doi.org/10.1128/mcb.00148-19 (2019).
46. Chen, G. et al. Monitoring TFEB translocation. *Methods Cell. Biol.* **164**, 1–9. https://doi.org/10.1016/bs.mcb.2020.10.017 (2021).
47. Napolitano, G. et al. mTOR-dependent phosphorylation controls TFEB nuclear export. *Nat. Commun.* **9**, 3312. https://doi.org/10.1038/s41467-018-05862-6 (2018).
48. J Klionsky, D. et al. Guidelines for the use and interpretation of assays for monitoring autophagy. *Autophagy* **17**, 1–382. https://doi.org/10.1080/15548627.2020.1797280 (2021).
49. Wang, Y. et al. Degradation of TRPML1 in neurons reduces Neuron Survival in transient global cerebral ischemia. *Oxidative Med. Cell. Longev.* **2018** (4612727). https://doi.org/10.1155/2018/4612727 (2018).
50. Yuyuan, L. et al. Downregulation of histone H4 lysine 16 acetylation ameliorates autophagic flux by resuming lysosomal functions in ischemic neurons. *ACS Chem. Neurosci.* **14**, 1834–1844. https://doi.org/10.1021/acschemneuro.3c00049 (2023).
51. Deng, Z. et al. LncRNA SNHG14 promotes OGD/R-induced neuron injury by inducing excessive mitophagy via miR-182-5p/BINP3 axis in HT22 mouse hippocampal neuronal cells. *Biol. Res.* **53**, 38. https://doi.org/10.1186/s40659-020-00304-4 (2020).
52. Hui, L. et al. Acidifying endolysosomes prevented low-density lipoprotein-induced amyloidogenesis. *J. Alzheimer's Disease: JAD* **67**, 393–410. https://doi.org/10.3233/jad-180941 (2019).
53. Xing, Y. et al. Blunting TRPML1 channels protects myocardial ischemia/reperfusion injury by restoring impaired cardiomyocyte autophagy. *Basic Res. Cardiol.* **117** https://doi.org/10.1007/s00395-022-00930-x (2022).
54. Zhang, M. et al. TMEM175 mediates lysosomal function and participates in neuronal injury induced by cerebral ischemia-reperfusion. *Mol. Brain* **13**, 113. https://doi.org/10.1186/s13041-020-00651-z (2020).
55. Chen, J. et al. Therapeutic benefit of intravenous administration of bone marrow stromal cells after cerebral ischemia in rats. *Stroke* **32**, 1005–1011. https://doi.org/10.1161/01.str.32.4.1005 (2001).

Author contributions

Q.L., X.C., Y.X., H.H. and Y.D. wrote the main manuscript text and these authors contributed equally to this work; X.C. and Q.L. Collected and processed experimental data; Q.L. prepared all figures; S.L. and J.W. modified the manuscript text; H.H. and Y.D. participated in the design of the study and supervised the progress of this research. All authors reviewed the manuscript. All authors have seen and approved the final version of the manu-

script being submitted. We warrant that the article is the author's original work, hasn't received prior publication, and isn't under consideration for publication elsewhere.

Funding
This work was supported by grants from the National Natural Science Foundation of China (Nos. 82160240 and 82160241), and Yunnan Talents Support Plan (No.YNWR-QNBJ-2018-034), and The innovation team of Stress and Disorder in Nervous System in Yunnan Province (No. 202305AS350011).

Declarations

Competing interests
The authors declare no competing interests.

Ethics approval and consent to participate
This study was approved by the Institutional Research Ethics Committee of Kunming University of Science and Technology (Appr.No.PZWH(滇)K2023-0053).

Additional information
Supplementary Information The online version contains supplementary material available at https://doi.org/10.1038/s41598-024-75802-6.

Correspondence and requests for materials should be addressed to H.H. or Y.D.

Reprints and permissions information is available at www.nature.com/reprints.

Publisher's note Springer Nature remains neutral with regard to jurisdictional claims in published maps and institutional affiliations.